



Pergamon

Ocean Engineering 27 (2000) 801–821

**OCEAN
ENGINEERING**

www.elsevier.com/locate/oceaneng

Model study of a shoreline wave-power system

Ruo-Shan Tseng^{a,*}, Rui-Hsiang Wu^a, Chai-Cheng Huang^b

^aDepartment of Marine Resources, National Sun Yat-Sen University, Kaohsiung, Taiwan, ROC 804

^bDepartment of Marine Environment, National Sun Yat-Sen University, Kaohsiung, Taiwan, ROC 804

Received 4 December 1998; accepted 4 March 1999

Abstract

A wave-power system which combines the concept of a breakwater and a harbor resonance chamber was developed in this study. In the caisson chamber, a multi-resonant oscillating water column (MOWC) was formed to push or suck air through the air turbine and thus continuously generated the power. The proposed wave-power system has two aims in mind: one is shore protection and the other is to extract energy from the ocean. To achieve an optimal effect of harbor resonance when excited by incident waves of various periods, a 60° opening of the cylindrical chamber with an entrance section and an arc-shaped curve board in front of the caisson was designed. In order to assess the energy-conversion efficiency and the hydraulic performance, a 1/20 model of this system was constructed and tested in the wave tank under various wave conditions. Our experimental data for the amplification factor of the MOWC agree well with previous theoretical results [Lee, J.J., 1971. *Journal of Fluid Mechanics* 45, 375–394]. The curve board proves to be useful: it not only broadens the resonant period but also increases the energy-extraction rate. The reflection coefficient was found to be generally low and to decrease with increasing wave height. However, due to the relatively high energy loss of the MOWC, only 28.5% of the incident-wave energy was converted into air energy, indicating that there are still areas for further improvement. In any event, the experimental results provided a clear picture of the energy-transformation process, and demonstrated the preliminary feasibility of this wave-energy device. © 2000 Elsevier Science Ltd. All rights reserved.

Keywords: Wave energy; Hydraulic model; Amplification coefficient; Oscillating water column

* Corresponding author. Tel.: + 886-7-5252-000 ext. 5033; fax: + 886-7-5255-033; e-mail: rstseng@mail.nsysu.edu.tw

1. Introduction

Ocean energy is considered as a viable alternative and renewable source of clean energy in many ocean countries. It consists of the so-called ocean thermal energy conversion (OTEC), tidal energy, wave energy and the energy from marine currents, etc. Initial considerations suggest that the OTEC system is not likely to be cost-effective in the near future. On the other hand, the tidal range of many coastal areas is not large enough for power production, and the energy density and extraction efficiency of marine currents may be too low to be utilized. Therefore, it is the wave-energy system that has the advantage of simple development technique and low capital cost, and can be considered as the first marine-energy resource that may be established for possible commercial production.

For many years, scientists and engineers have been constantly working to develop an effective device for the utilization of ocean-wave energy. A variety of wave-energy extraction devices have been invented mainly in Japan, the UK, the USA, Norway and some other countries. These range widely in sophistication. The devices for harnessing wave energy may be classified into four groups: propulsion schemes, buoy power-supply devices, offshore power plants and shore-based power stations. Reviews of much of this research can be found in Constans (1979); Shaw (1982); Carmichael and Falnes (1992). Among the various wave-energy converters, the oscillating water column (OWC) is generally considered to be one of the most promising; they have been successfully constructed and tested at a number of sites. An example is the Japanese project “KAIMEI”, which is shaped like a ship and was designed to explore the production of electricity by way of OWC devices. KAIMEI was tested at sea from 1979 to 1987. The first wave-power station in Britain has been operational on the Isle of Islay, off the west coast of Scotland, since 1990. The working principle of this system is also based on the OWC type to drive a 75 kW Wells turbine/generator unit (Whittaker et al., 1993; Muller and Whittaker, 1995). The OWC consists of a partially submerged chamber with an opening in the front through which waves force the water in the chamber to oscillate. The air is forced by the oscillating body of water to leave and enter the chamber through an air turbine, thus extracting energy from the waves. Evans et al. (1995) conducted numerical modeling to predict the optimal geometry and power take-off parameters of an OWC. Whittaker and Stewart (1993) have done experimental investigations into the performance of the OWC when incorporated with rectangular or tapered harbors. They concluded that the maximum power output is increased by a factor of two if the same OWC is embedded in a fully reflecting coastline. An OWC system with two projecting parallel side walls is called a multi-resonant OWC (MOWC), and was shown to be more efficient in absorbing wave energy for a wide bandwidth frequency (Ambli et al., 1982). Thiruvankatasamy and Neelamani (1997) conducted laboratory investigations on the efficiency of power absorption of MOWC wave-energy caissons in an array. It was found that the hydrodynamic efficiency of the MOWC increases with increasing s/b value up to 3, where s is the spacing between caissons and b is the OWC width. In Norway, a wave-power plant based on the MOWC principle with a maximum capacity of 500 kW has been operating since 1985, and is now

feeding electricity to the local grid. Based on the MOWC principle, a prototype wave-power plant has been installed off Trivandrum on the west coast of India with a combination of the wave-power converter and the caisson-type breakwater.

In Taiwan, rapid industrial growth also means rapid growth of power demand. According to a report by the Energy Commission, the per capita consumption of energy grew by 6.5% annually between 1971 and 1991, and the trend is expected to continue. In the pursuit of generating power in harmony with the environment, Taiwan Power Company has conducted several programs into the development of alternative energy. One of the programs of alternative energy development is wave power. It is not difficult to see why wave power comes naturally to Taiwan. While it is beset with problems of pollution and land shortages, Taiwan has abundant wave-energy resources practically in its own backyard. However, there have been only a few studies on the utilization of ocean energy in Taiwan, such as the artificial upwelling system by which cold, deep seawater can be surfaced for mariculture or OTEC uses (Liang et al., 1978; Liang, 1996). On the other hand, the potential of wave power along the Taiwan coast and a feasibility study of wave-power development were examined by Wu et al. (1986), but no laboratory or field testing has been reported yet. The purpose of this study is, therefore, to develop a physical model of the wave-power system based on the actual wave statistics along the Taiwan coast. Model test results of this wave-power system are reported here in this paper.

2. System design of a wave-energy convertor

A wave-energy device, which is particularly suitable for (but not limited to) the wave conditions around the Taiwan coast, is developed in the present study. From a literature review on the existing wave-power systems in Norway, the UK, Japan and some other countries, it was decided in this study to adopt the concept of the oscillating water column in a pneumatic-type wave-energy conversion system. This system is characterized by air chambers around a cylindrical caisson, so that wave energy incident from various directions could be utilized efficiently and a wide, calm sea area can also be provided behind the system. In other words, this system is designed to have both functions of wave-power extraction and shore protection. In order to investigate the flow conditions and conversion efficiencies of this wave-energy device, a physical, hydraulic model was constructed and tested in the wave tank.

To increase the energy extraction efficiency of the wave-power device, the amplification factor of the wave amplitude inside the caisson chamber should be designed to be as large as possible. This problem is similar to the phenomenon of harbor resonance when excited by incident waves. Lee (1971) developed a theory for the wave-induced oscillations in harbors of arbitrary geometry (with constant depth), and his theoretical results also agreed well with experimental data for circular harbors with 10° and 60° openings. For the harbor with a 60° opening it was found that the amplification of the wave amplitude inside the harbor was smaller, but the band widths of wavenumbers for each resonance mode were wider, than in the case of

the 10° opening. The results of Lee (1971) also indicated that the effect of viscous dissipation became more important for the harbor with a smaller opening. Taking all these factors into consideration, a 60° opening was thus selected for the cylindrical caisson in this study [Fig. 1(a)]. The conceptual design of this wave-power system is illustrated in the flowchart of Fig. 1. The cylinder has a 60° opening on the section below the water surface but is closed on the top portion to allow air passage [Fig. 1(b)]. This cylinder is enclosed in a rectangular-shaped caisson which serves as a breakwater. Two boards extending from the cylindrical opening to two sides of the caisson form a wave entrance section [Fig. 1(c)], which was designed to concentrate the energy of incident waves into the cylinder by reflection effects. On top of the entrance was mounted an arc-shaped curve board [Fig. 1(d)]. This curve board, which aims to improve the performance of the wave-power device, is a unique design in our system and its function will be tested and discussed further in this paper. The air flow induced by the rise and fall of the MOWC inside the caisson chamber drives an air turbine [Fig. 1(e)], which rotates in the same direction irrespective of the direction of the air flow. Speaking overall, the working principle of this system, as illustrated in Fig. 2, is to convert the kinetic and potential energy of the undulating ocean surface into mechanical energy of the air turbine.

The design criteria for this wave-power converter were based on the actual wave statistics around the Taiwan coast. According to Chang (1993), the most possible conditions of significant waves can be summarized as the following: wave height range is 0.7–4 m, wave period range is 6–12 s, and the selected water depth range for this system is 8–12 m. The optimal size of the cylindrical caisson can be determined from the results of Lee (1971), which indicated that the amplification factor at the lowest mode is of the order of 3, with the magnitude of ka at resonance about 0.5; i.e.

$$ka = \frac{1}{2} \text{ or } a = \frac{L}{4\pi}, \quad (1)$$

where a is the radius of the cylindrical caisson, k is the wavenumber and L is the wave length. Assuming the caisson is situated at the water depth of 12 m and the wave period is 8 s, then the wave length derived from the dispersion relationship is 75.8 m. As a result, the optimal radius of the prototype cylindrical caisson which produces the largest resonance effect is approximately 6 m.

3. Hydraulic model testing

The hydraulic experiments were conducted in a wave tank, 35 m long, 1 m wide and 1.2 m high, that has two transparent side walls. The water depth is 60 cm. At 22 m downstream from the piston wave maker, a 1/20 scale model of the wave-power station was placed on the tank bottom. The model consists of two parts: a rectangular caisson chamber and an air turbine on top of the chamber. A hollow cylinder with a diameter of 60 cm and a 60° opening on the front was contained inside the caisson. This caisson was made from stainless steel and weighed about

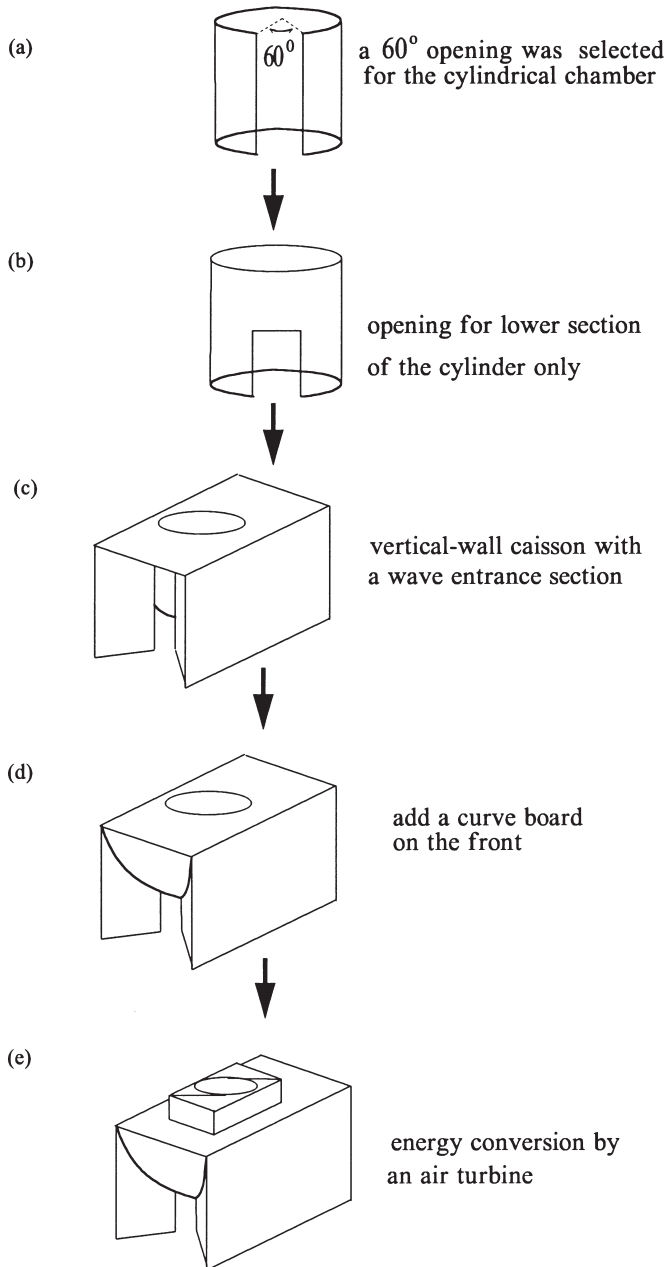


Fig. 1. Conceptual design flowchart of the wave-power system.

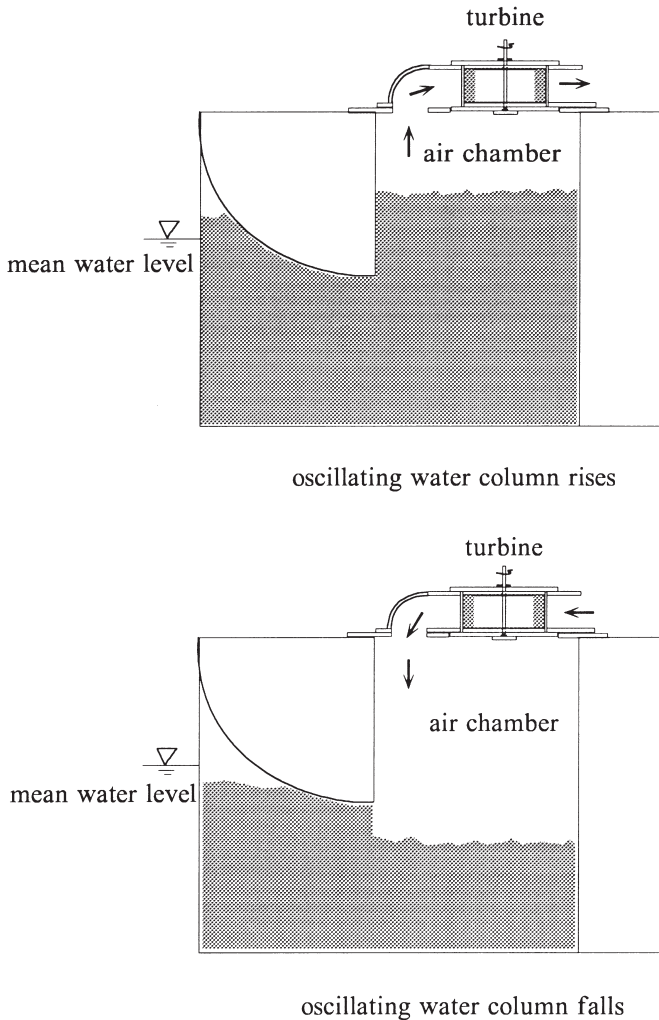


Fig. 2. Working principle of the wave-power system.

94 kg. A curve board and an entrance section were installed on the front of this caisson (Fig. 3). On top of the caisson is a 48-blade air turbine, which is made of transparent Plexiglass combined with poly(vinyl chloride) blades, a copper fly wheel, a stainless steel shaft and some bearing parts, etc. Three capacitance wave gages were used in this study to monitor the water-surface elevations at different locations. Two wave gages were placed at 2.5 m and 2 m in front of the model, to estimate the reflection coefficient, and one wave gage was mounted inside the caisson to detect its amplification effect. Analog signals from the wave gages were digitized at a 40 Hz sampling rate by the data-acquisition system before feeding into a personal computer. Note that there is an orifice in both the front and the back of the air

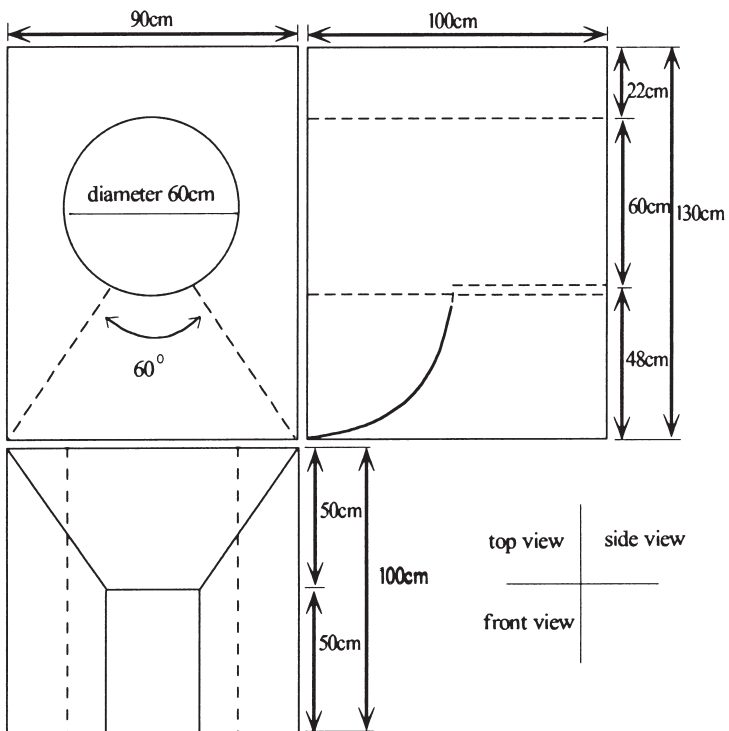
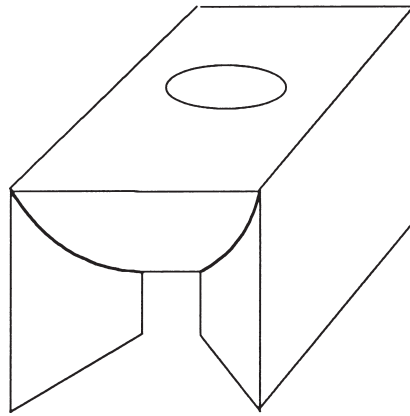


Fig. 3. General views of the resonant caisson.

turbine to allow air to enter or escape from the chamber. Two Validyne differential pressure sensors were placed in the air chamber and the front orifice of the air turbine to measure their air pressure difference with respect to the outside air. On the shaft of the air turbine was fastened an aluminum thread roller of 3 cm radius with a load of various weights to measure the output power and the static and dynamic frictional force of the air turbine. The experimental set-up of this study is presented in Fig. 4. Plates 1 and 2 show the caisson model and the complete wave-power system, respectively.

The experimental conditions of this study, as shown in Table 1, consists of seven different wave periods and four different wave heights. Note that kinematic similarity exists between the model and prototype, and their Froude numbers are set to be equal. The experiments were also conducted for the conditions of with/without the curve board in front of the caisson. The experiments were performed using the following procedures:

1. Wave-energy transformation for the case of caisson only (without air turbine): data were collected and analyzed for five waves in the steady-state condition.
2. Wave-energy transformation for the case of caisson plus air turbine: same procedures and measurements were made as for the first case except that air pressure data were also collected.
3. Measurements of the air turbine output power: in this case, a load of a certain weight was connected to the thread roller. The time for this load to travel up a

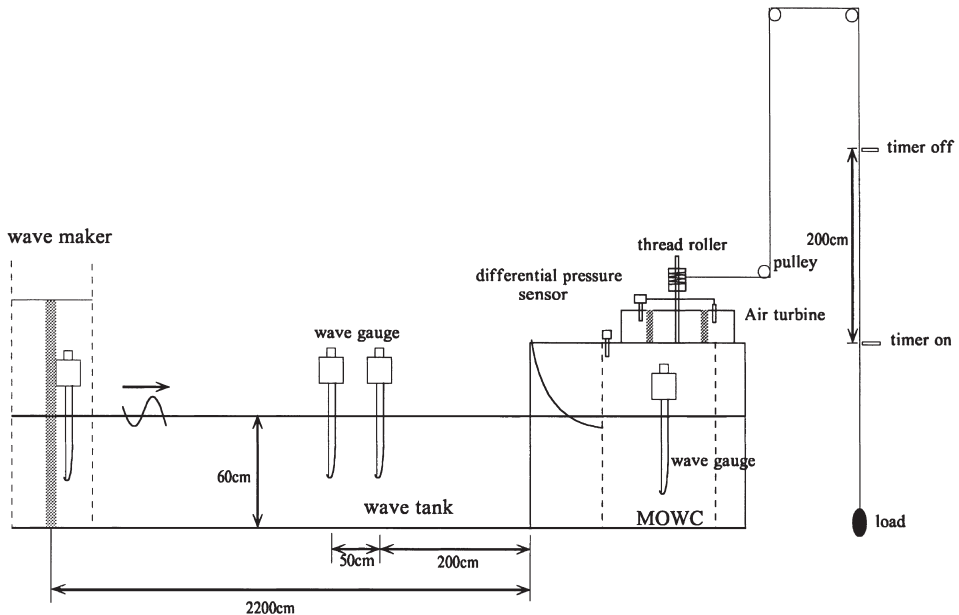


Fig. 4. Experimental set-up.

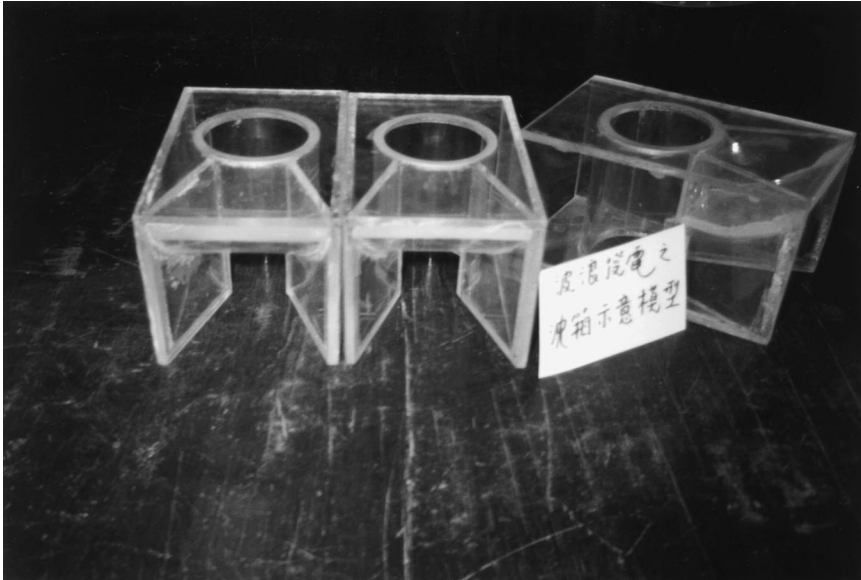


Plate 1. Resonant caisson model.

vertical distance of 2 m for a certain wave condition was measured by a timer and a micro switch (Fig. 4).

4. Results and discussion

4.1. Wave-energy transformation for the case of caisson only (without air turbine)

According to the law of energy conservation, the amount of wave energy entering the caisson will be equal to the sum of that energy leaving the caisson plus the energy stored in the system and the energy loss; i.e.,

$$E_I = E_R + E_W + E_L, \quad (2)$$

where E_I is the incident-wave energy, E_R is the reflected-wave energy, E_W is the wave energy of the MOWC in the caisson and E_L is the frictional energy loss due to viscosity and turbulent motion of the flow. The total energy per wave per unit width can be expressed as (Dean and Dalrymple, 1993):

$$E = 1/8\rho gH^2L, \quad (3)$$

where ρ is the water density, g is the gravitational acceleration, H is the wave height and L is the wave length. The width of the model caisson is 0.9 m (Fig. 3). On the other hand, the waves reflected from the caisson are acting on the 1 m wide wave tank. Therefore, the ratio of the reflected-wave energy to the incident-wave energy is:

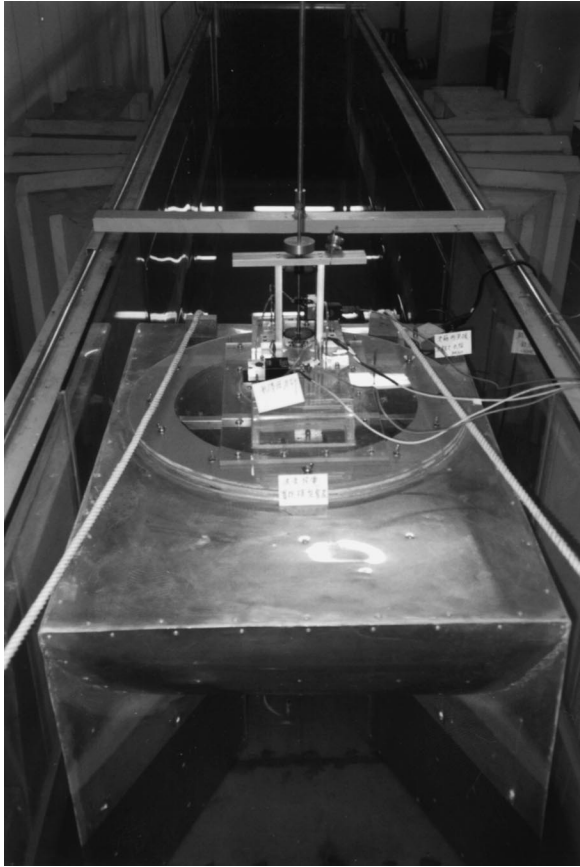


Plate 2. Wave-power system.

Table 1
The experimental conditions

Wave period (s)	1.34, 1.57, 1.79, 2.01, 2.24, 2.46, 2.68
Wave height (cm)	5, 6, 8, 10
Water depth (cm)	60
Number of turbine blades	48
Caisson curve board	With and without
Air turbine	With and without

$$\frac{E_R}{E_I} = \frac{1/8\rho g H_R^2 L \times 1}{1/8\rho g H_I^2 L \times 0.9} = \frac{1}{0.9} \left(\frac{H_R}{H_I} \right)^2 = \frac{1}{0.9} K_R^2, \quad (4)$$

where H_R and H_I are the heights of the incident and reflected waves, respectively, and K_R is the reflection coefficient. The method of Goda and Suzuki (1976) was

adopted in this study to derive the value of K_R . They obtained theoretical solutions of the reflection coefficient based on the linear water-wave theory and measurements of water-surface elevations by two wave gages a fixed distance apart.

The wave energy of the MOWC inside the caisson chamber consists of the potential energy of the undulating water surface only and can be expressed as:

$$E_w = 1/16\rho g H_w^2 \pi a^2, \tag{5}$$

where H_w is the wave height of the MOWC and a is the radius of the caisson (30 cm). As a result, the efficiency of the wave-energy extraction is:

$$\frac{E_w}{E_1} = \frac{1/16\rho g H_w^2 \pi \times (0.3)^2}{1/8\rho g H_1^2 L \times 0.9} = 0.05 \pi R^2/L, \tag{6}$$

where $R = H_w/H_1$ is the amplification factor (or coefficient) of the MOWC.

Experimental results for the reflection and amplification coefficients as functions of wave period and wave height with no curve board present are shown in Figs. 5 and 6, respectively. The minimum reflection coefficient occurs at a wave period of 1.79 s, which corresponds to ocean waves of 8 s period and is also the designed natural period of oscillation of the caisson chamber itself. It is also found that the reflection coefficient generally decreases with increasing wave height. The amplification coefficient has a maximum value of 2.1–2.6 for various wave heights at the wave period of 1.79 s. Table 2 gives the percentage for each transformed component of the incident-wave energy with no curve board present as functions of wave period and wave height. It can be seen that, at the wave period of 1.79 s, the efficiency of wave-energy extraction has a maximum value and it increases from 19.52% to 27.16% with increasing wave height. The amount of energy loss tends to decrease with increasing wave period, but the relationship with the wave height is not clear.

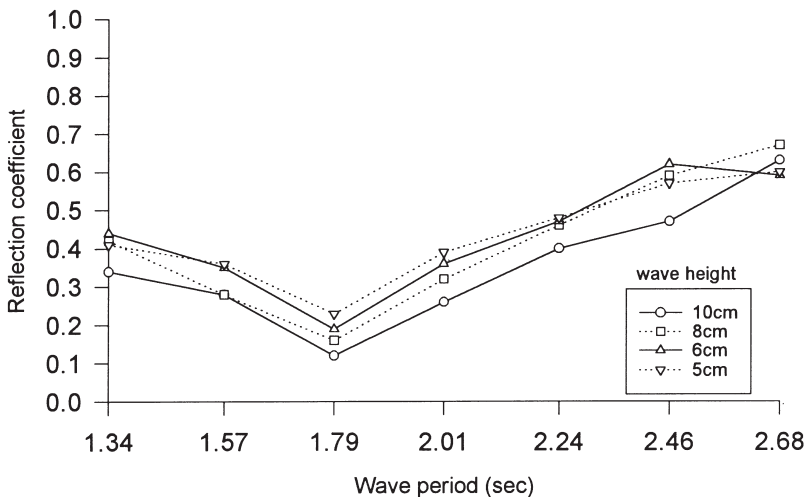


Fig. 5. Reflection coefficient of the caisson with no curve board present.

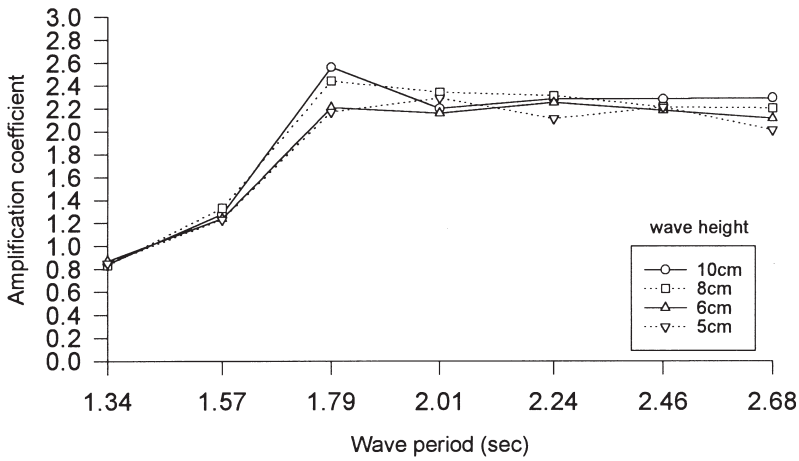


Fig. 6. Amplification coefficient of the caisson with no curve board present.

Table 2

Percentage of incident-wave energy in each transformed component for various wave conditions with no curve board present

Wave height (cm)		Wave period (s)						
		1.34	1.57	1.79	2.01	2.24	2.46	2.68
10	Incident-wave energy (%)	100	100	100	100	100	100	100
	Reflected energy	12.84	8.71	1.60	7.51	17.78	24.54	44.10
	MOWC energy	4.36	8.12	27.16	17.32	16.36	14.66	13.42
	Energy loss	82.80	83.17	71.24	75.17	65.86	60.80	42.48
8	Incident-wave energy (%)	100	100	100	100	100	100	100
	Reflected energy	19.60	8.71	2.84	11.38	23.51	38.68	49.88
	MOWC energy	4.26	8.77	24.68	19.59	16.80	13.65	12.38
	Energy loss	76.14	82.52	72.48	69.03	59.69	47.67	37.74
6	Incident-wave energy (%)	100	100	100	100	100	100	100
	Reflected energy	21.51	13.61	4.01	14.40	24.54	42.71	38.68
	MOWC energy	4.68	7.62	20.24	16.69	15.94	13.40	11.39
	Energy loss	73.81	78.77	75.75	68.91	59.52	43.89	49.93
5	Incident-wave energy (%)	100	100	100	100	100	100	100
	Reflected energy	18.68	14.40	5.88	16.90	25.60	36.10	40.00
	MOWC energy	4.47	7.50	19.52	18.76	14.02	13.77	10.34
	Energy loss	76.85	78.10	74.60	64.34	60.38	50.13	49.66

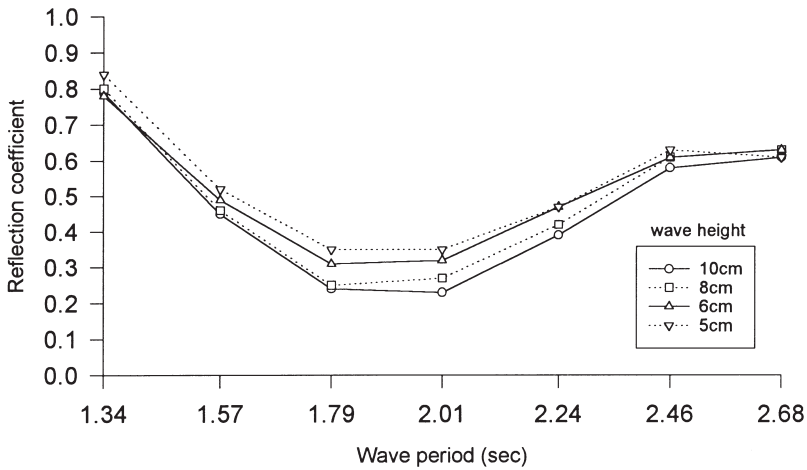


Fig. 7. Reflection coefficient of the caisson with the curve board present.

The reflection and amplification coefficients as functions of wave period and wave height with the curve board present are plotted in Figs. 7 and 8, respectively. Table 3 shows the percentage for each transformed component of the incident-wave energy with the curve board present as functions of wave period and wave height. It can be seen from Fig. 7 that the minimum reflection coefficient occurs at the wave period of 1.79–2.01 s. However, the reflection coefficient generally becomes larger with the curve board present than without for the same wave conditions. Note that the amplification coefficient is larger for smaller wave heights at the wave period of 1.79–2.24 s (Fig. 8). Fig. 9 is a comparison of the amplification coefficient versus the wavenumber parameter ka (where k is the wavenumber and a is the radius of

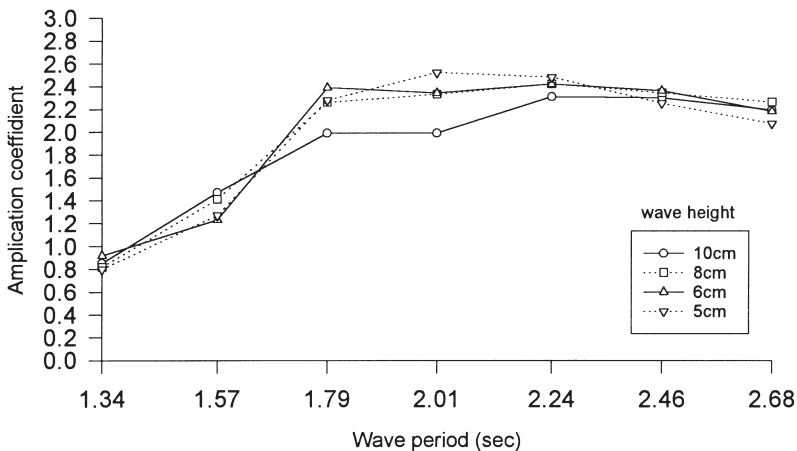


Fig. 8. Amplification coefficient of the caisson with the curve board present.

Table 3

Percentage of incident-wave energy in each transformed component for various wave conditions with the curve board present

Wave height (cm)		Wave period (s)						
		1.34	1.57	1.79	2.01	2.24	2.46	2.68
10	Incident-wave energy (%)	100	100	100	100	100	100	100
	Reflected energy	69.34	22.50	6.40	5.88	16.90	37.38	41.34
	MOWC energy	4.47	10.71	16.41	14.17	16.80	14.92	12.27
	Energy loss	26.19	66.79	77.19	79.95	66.30	47.70	46.39
8	Incident-wave energy (%)	100	100	100	100	100	100	100
	Reflected energy	71.11	23.51	6.94	8.10	19.60	41.34	44.10
	MOWC energy	4.16	9.85	21.17	19.43	18.44	15.44	13.07
	Energy loss	24.73	66.64	71.89	72.47	61.96	43.22	42.83
6	Incident-wave energy (%)	100	100	100	100	100	100	100
	Reflected energy	67.60	26.68	10.68	11.38	24.54	41.34	44.10
	MOWC energy	5.24	7.50	23.67	19.59	18.44	15.71	12.16
	Energy loss	27.16	65.82	65.65	69.03	57.02	42.95	43.74
5	Incident-wave energy (%)	100	100	100	100	100	100	100
	Reflected energy	78.40	30.04	13.61	13.61	24.54	44.10	41.34
	MOWC energy	3.96	7.99	21.55	22.72	19.36	14.28	10.96
	Energy loss	17.64	61.97	64.84	63.67	56.10	41.62	47.70

the circular chamber) between our experimental results of with/without the curve board and the theoretical predictions of Lee (1971). Most of our experimental data are concentrated at the first mode of resonant oscillations with the range of ka between 0.3 and 0.8. It can be seen that our experimental data agree well with the theoretical results. Except for a few data points, the amplification coefficients for the case with the curve board present are slightly greater than for the case without. This indicates that the function of the curve board is twofold: one is to increase the amplification coefficient and the energy-extraction rate of the MOWC under small-wave conditions, the other is to broaden the resonant period so that incident waves of a wider range of periods can be utilized.

4.2. Wave-energy transformation for the case of caisson plus air turbine

In this part of the work, a 48-blade air turbine was installed on top of the caisson chamber to convert the wave energy into mechanical energy. The energy conservation law of Eq. (2) is now modified to the following form:

$$E_I = E_R + E_W + E_A + E_L, \quad (7)$$

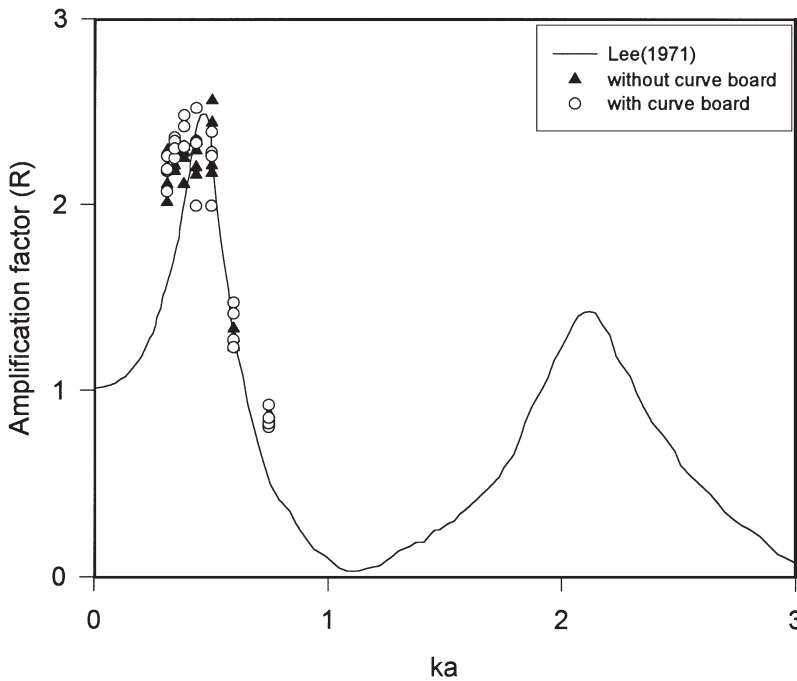


Fig. 9. Response curve of the cylindrical chamber with and without the curve board present. The solid line is the theoretical results of Lee (1971).

where E_A is the stored energy in the air chamber on top of the MOWC and can be obtained by:

$$E_A = \int_0^T \Delta P_a Q dt, \tag{8}$$

where ΔP_a is the total pressure difference between the inside and outside of the air chamber and Q is the volume flow rate of air, derived by taking differentiation of the volume of the oscillating water column with respect to time. The stored energy in the air chamber is then further divided into two parts: the effective input energy, E_{ti} , and the exhaust air energy, E_{te} . The effective turbine input energy can be estimated by:

$$E_{ti} = \int_0^T \Delta P_t Q dt, \tag{9}$$

where ΔP_t is the total pressure difference between the inlet and outlet orifices of the turbine. Subsequently, E_{te} can be obtained by subtracting E_{ti} from E_A . The reflection and amplification coefficients as functions of wave period and wave height with the

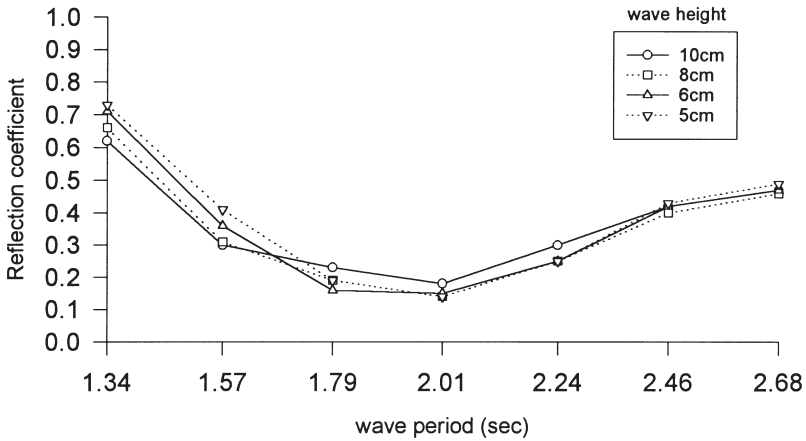


Fig. 10. Reflection coefficient of the caisson with the curve board and air turbine present.

curve board and air turbine present are presented in Figs. 10 and 11, respectively. Both the reflection and amplification coefficients decrease more with the air turbine present than without. The amplification coefficient is also found to be larger for smaller wave heights, and the reflection coefficient has minimum values at the wave period of 1.79–2.01 s. Plotted in Fig. 12 is the water-surface elevation inside the caisson chamber, Q , ΔP_a , ΔP_t , \dot{E}_A and \dot{E}_i with respect to time for a typical experiment of 10 cm wave height and 2.01 s wave period, where \dot{E}_i and \dot{E}_A represent the power. Note that \dot{E}_i and \dot{E}_A are in phase, and their period of oscillation is only half the period of the incident waves. Table 4 shows the percentage for each transformed component of the incident-wave energy with the curve board and air turbine present

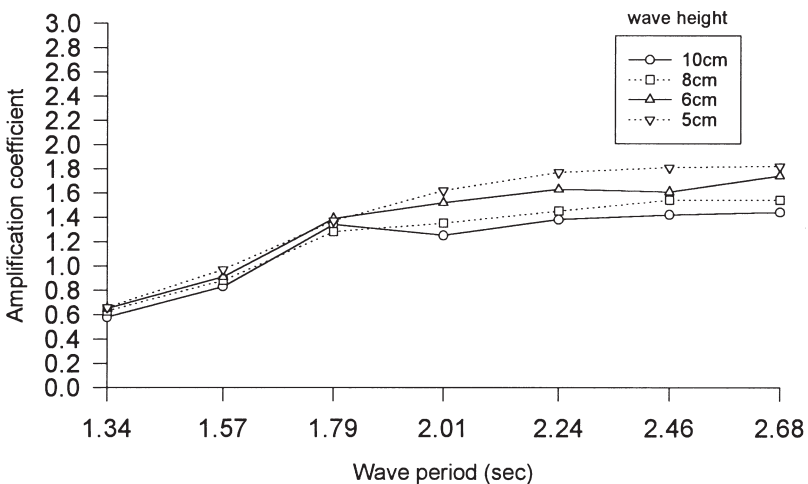


Fig. 11. Amplification coefficient of the caisson with the curve board and air turbine present.

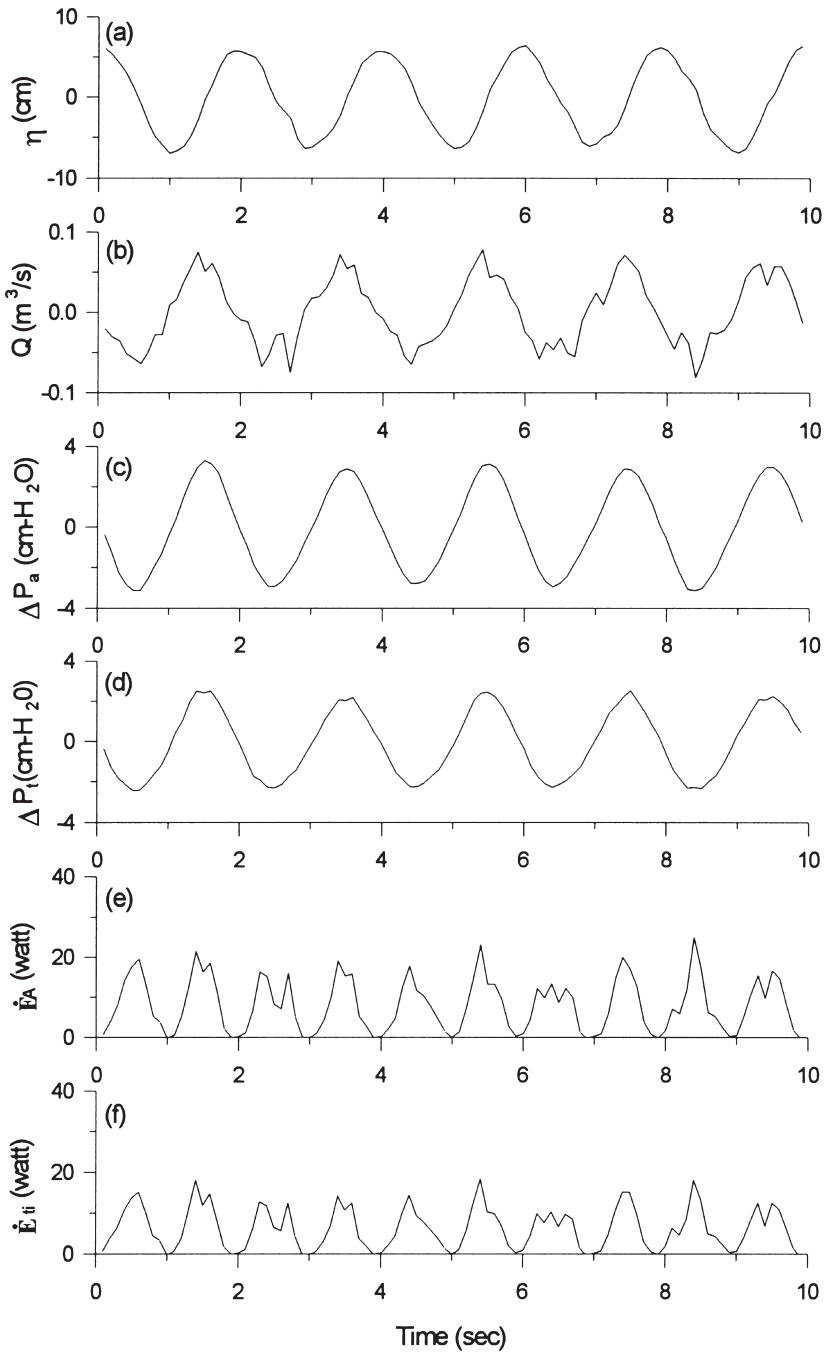


Fig. 12. (a) Water-surface elevation in the MOWC; (b) Q ; (c) ΔP_a ; (d) ΔP_i ; (e) \dot{E}_a and (f) \dot{E}_i when the caisson chamber and air turbine were incorporated under the condition of 10 cm wave height and 2.01 s wave period.

Table 4

Percentage of incident-wave energy in each transformed component for various wave conditions with the curve board and air turbine present

Wave height (cm)		Wave period (s)						
		1.34	1.57	1.79	2.01	2.24	2.46	2.68
10	Incident-wave energy (%)	100	100	100	100	100	100	100
	Reflected energy	42.71	10.00	5.88	3.60	10.00	19.60	24.54
	MOWC energy	2.08	3.42	7.44	5.59	6.00	5.69	5.31
	Air energy	10.10	20.17	30.34	33.53	31.19	26.80	21.35
	Effective energy	7.89	15.73	23.92	26.57	24.86	21.08	16.80
	Exhaust energy	2.21	4.44	6.42	6.96	6.33	5.72	4.55
	Energy loss	45.11	66.41	56.34	57.28	52.81	47.91	48.80
8	Incident-wave energy (%)	100	100	100	100	100	100	100
	Reflected energy	48.40	10.68	4.01	2.18	6.94	17.78	23.51
	MOWC energy	2.46	3.84	6.79	6.52	6.62	6.69	6.07
	Air energy	8.16	19.06	27.87	31.62	27.81	25.31	18.57
	Effective energy	6.37	14.95	21.56	24.65	21.75	19.84	14.35
	Exhaust energy	1.79	4.11	6.31	6.97	6.06	5.47	4.22
	Energy loss	40.98	66.42	61.33	59.68	58.63	50.22	51.85
6	Incident-wave energy (%)	100	100	100	100	100	100	100
	Reflected energy	56.01	14.40	2.84	2.18	6.94	19.60	24.54
	MOWC energy	2.61	4.10	8.01	8.27	8.37	7.31	7.75
	Air energy	5.60	15.34	24.07	30.82	24.56	18.53	14.78
	Effective energy	4.25	11.74	18.37	23.60	18.90	14.35	11.46
	Exhaust energy	1.35	3.60	5.70	7.22	5.66	4.18	3.32
	Energy loss	35.78	66.16	65.08	58.73	60.13	54.56	52.93
5	Incident-wave energy (%)	100	100	100	100	100	100	100
	Reflected energy	59.21	18.68	4.01	2.50	6.94	20.54	26.68
	MOWC energy	2.70	4.66	7.78	9.39	9.86	9.24	8.48
	Air energy	5.14	11.21	20.48	29.18	24.84	19.90	13.39
	Effective energy	3.96	8.77	16.14	22.17	19.13	15.38	10.33
	Exhaust energy	1.18	2.44	4.34	7.01	5.71	4.52	3.06
	Energy loss	32.95	65.45	67.73	58.93	58.36	50.32	51.45

as functions of wave height and wave period. It can be seen from Table 4 that the reflected-wave energy has minimum values at the wave period of 1.79–2.01 s, and the value is lower than that without the air turbine present (Table 3). The wave energy of the MOWC is smaller with the air turbine present than without, apparently because part of the energy is converted into air energy. The maximum air-energy extraction rate is around 33.5%, which occurs at the wave period of 2.01 s rather than the preset period of 1.79 s. At the wave period of 1.79–2.01 s, the energy-loss rate decreases with the air turbine present. It is inferred that the amplitude of the

MOWC becomes smaller with the air turbine present, which results in the reduction of turbulent frictional loss as a consequence.

4.3. Extraction efficiency of wave energy

The energy-transformation processes with and without the air turbine present are plotted in Fig. 13 for the average results of various conditions under two wave periods (1.79 and 2.01 s) and four wave heights (5, 6, 8 and 10 cm). For the case of with caisson chamber only but with no air turbine present, the 100% incident-wave energy was converted into reflected-wave energy (9.6%), the wave energy of MOWC (19.8%) and energy loss (70.6%). When the caisson chamber was incorporated with the 48-blade air turbine, some of the incident-wave energy was partitioned to the stored energy of the air chamber (28.5%) on top of the MOWC. At the same time

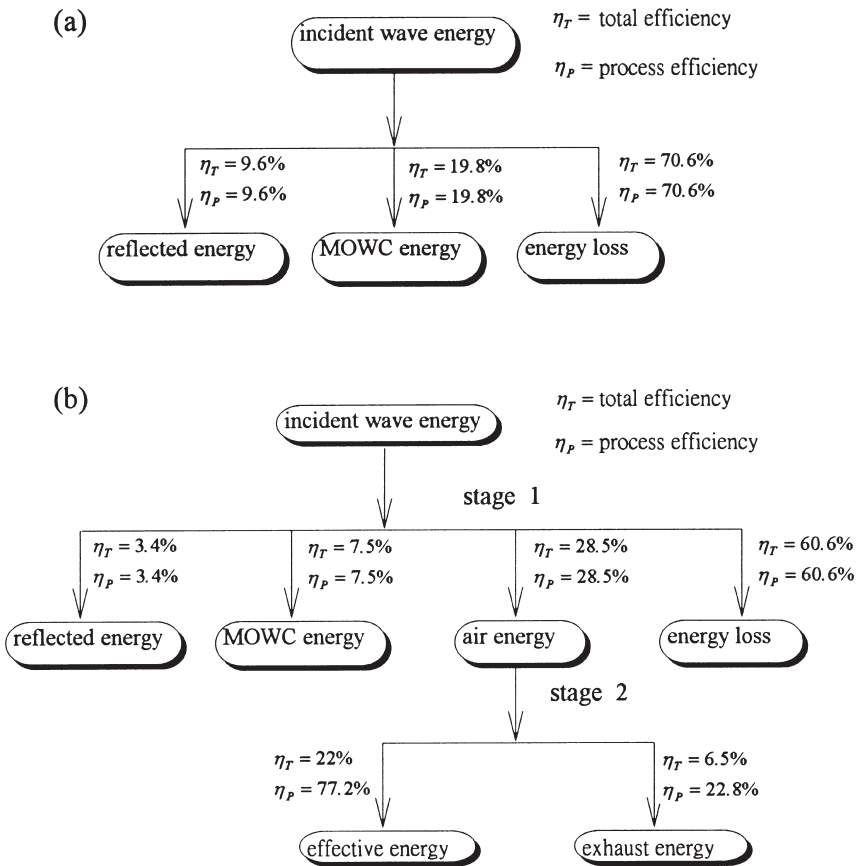


Fig. 13. Wave-energy transformation process and energy-extraction efficiency in each stage and component for cases of (a) without and (b) with the air turbine present (average results of $T = 1.79$ and 2.01 s, $H = 5, 6, 8$ and 10 cm).

other parts of the energy were also reduced; i.e., the reflected-wave energy (3.4%), the wave energy of the MOWC (7.5%) and the energy loss (60.6%). This clearly indicated that the stored energy of the air chamber with the air turbine present, which is the useful product of this wave-energy system, came mainly from the wave energy of the MOWC but also derived partly from the reflected-wave energy and the energy loss with no air turbine present.

As mentioned earlier, the stored energy inside the air chamber (28.5%) was then divided into two parts: the effective turbine input energy (22%) and the turbine exhaust energy (0.5%), as seen from Fig. 12(b). Note that only part of the effective turbine input energy can be used to drive the turbine/generator, the rest is dissipated by mechanical friction. This represents a conversion efficiency of about 77% of the air turbine. This process can probably be improved in the future by using a more effective turbine such as the Japanese Wells air turbine.

5. Conclusions

A wave-power system, based on the working principle of a multiple-resonant oscillating water column of the pneumatic type, is developed in this study. The system is characterized by air chambers on top of a cylindrical caisson with an wave entrance section and an arc-shaped curve board on the front to improve the system performance. In order to investigate the flow conditions and energy-conversion efficiencies of the system, a 1/20 physical model was constructed and tested in the wave tank. Experiments were conducted for various wave periods and wave heights as well as for different caisson and turbine configurations. Water-surface elevations inside and outside the oscillating water column, as well as the pressure difference in the air chamber and the orifices of the air turbine, were monitored in order to estimate the energy-conversion efficiency of this system.

To achieve an optimal effect of wave-amplitude amplification in the caisson chamber, a 60° opening of the cylinder was selected, and our experimental data for the amplification factor agree well with the theoretical results of Lee (1971). The arc-shaped curve board in front of the caisson proves to be useful: it not only broadens the resonant period but also increases the energy-extraction rate for small wave heights. However, due to the relatively high energy loss of the MOWC, only 28.5% of the incident-wave energy was converted into air energy, indicating that further efforts are required in this area to improve the energy-extraction rate. The experimental results clearly demonstrate the feasibility and capability of this wave-energy device model, and at-sea tests will be conducted in the next stage of the work.

Acknowledgements

We thank the National Science Council for partly supporting this research (NSC85-2611-E-110-003).

References

- Ambli, N., Bonke, K., Malmo, O., Reitan, H., 1982. The Kvaerner multiresonant OWC. In: Proceedings of the 2nd International Symposium on Wave Energy Utilisation, Trondheim, Norway. Tapir, pp. 275–295.
- Carmichael, A.D., Falnes, J., 1992. State of the art in wave power recovery. In: Proceedings of the International Conference on Ocean Engineering, Recovery—State of the Art, ASCE.
- Chang, C.-K., 1993. Status and evaluation of wave measurements in Taiwan. In: Proceedings of the Conference on Marine Meteorology, Taipei, Taiwan, pp. 73–91 (in Chinese).
- Constans, J., 1979. Marine Sources of Energy. Pergamon Press, New York.
- Dean, R.G., Dalrymple, R.A., 1993. Water Wave Mechanics for Engineers and Scientists. World Scientific Publishing Co., Singapore.
- Evans, D.V., O’Gallachoir, B.P., Porter, R., Thomas, G.P., 1995. On the optimal design of an oscillating water column device. In: Proceedings of the Second European Wave Power Conference, Lisbon, Portugal, pp. 172–178.
- Goda, Y., Suzuki, Y., 1976. Estimation of incident and reflected wave in random experiment. In: Proceedings of the 15th Conference on Coastal Engineering, Hawaii, pp. 828–845.
- Lee, J.J., 1971. Wave-induced oscillations in harbours of arbitrary geometry. *Journal of Fluid Mechanics* 45, 375–394.
- Liang, N.K., Huang, P.A., Li, D.J., Chu, L.L., Wu, C.L., Liang, N.T., 1978. Artificial upwelling induced by ocean currents—theory and experiment. *Ocean Engineering* 5, 83–94.
- Liang, N.K., 1996. A preliminary study on air-lift artificial upwelling system. *Acta Oceanographica Taiwanica* 35, 187–200.
- Muller, G., Whittaker, T.J.T., 1995. Visualization of flow condition inside a shoreline wave power-station. *Ocean Engineering* 22, 629–641.
- Shaw, R., 1982. Wave Energy—A Design Challenge. Ellis Horwood Limited, UK.
- Thiruvenkatasamy, K., Neelamani, S., 1997. On the efficiency of wave energy caissons in array. *Applied Ocean Research* 19, 61–72.
- Whittaker, T.J.T., McIwaine, S.J., Raghunathan, S., 1993. A review of the Islay shoreline wave power station. In: Proceedings of the European Wave Energy Symposium, Edinburgh, Scotland, pp. 283–286.
- Whittaker, T.J.T., Stewart, T.P., 1993. An experimental study of nearshore and shoreline oscillating water columns with harbors. In: Proceedings of the European Wave Energy Symposium, Edinburgh, Scotland, pp. 151–156.
- Wu, F.H.Y., Leung, T.C.F., Tzong, T.Y., 1986. A hydraulic wave power system. In: Proceedings of 3rd International Symposium on Wave, Tidal, OTEC and Small Scale Hydra Energy, Brighton, UK, pp. 397–411.